

CMS Search Plans and Sensitivity to New Physics with Dijets

The CMS Collaboration

Abstract

1 CMS will use dijets to search for physics beyond the standard model during early LHC
2 running. The inclusive jet cross section as a function of jet transverse momentum, with 10
3 pb^{-1} of integrated luminosity, is sensitive to contact interactions beyond the reach of the
4 Tevatron. The dijet mass distribution will be used to search for dijet resonances coming
5 from new particles, for example an excited quark. Additional sensitivity to the existence
6 of contact interactions or dijet resonances can be obtained by comparing dijet rates in
7 two distinct pseudorapidity regions.

8 The Large Hadron Collider at CERN will produce many events with two energetic jets
9 resulting from proton-proton collisions at $\sqrt{s} = 14$ TeV. These dijet events result from
10 parton scattering, produced by the strong interaction of quarks (q) and gluons (g) inside
11 the protons. This paper discusses plans to use dijets in the search for two signals of new
12 physics: contact interactions and resonances decaying into dijets. This generic search is
13 applied to two models of quark compositeness, that are used as benchmarks of sensitivity
14 to new physics. The first model is a contact interaction [1] among left-handed quarks
15 at an energy scale Λ^+ in the process $qq \rightarrow qq$, modeled with the effective Lagrangian
16 $L_{qq} = (\pm 2\pi/\Lambda^2)(\bar{q}_L\gamma^\mu q_L)(\bar{q}_L\gamma_\mu q_L)$ with $+$ chosen for the sign. The second model is an
17 excited quark (q^*) [2] in the process $qg \rightarrow q^* \rightarrow qg$, detectable as a dijet resonance. All
18 processes presented here have been simulated using PYTHIA version 6.4 [3].

19 A detailed description of the Compact Muon Solenoid (CMS) experiment can be found
20 elsewhere [4, 5]. The CMS coordinate system has the origin at the center of the detector,
21 z -axis points along the beam direction toward the west, with the transverse plane per-
22 pendicular to the beam. We define ϕ to be the azimuthal angle, θ to be the polar angle
23 and the pseudorapidity as $\eta = -\ln(\tan[\theta/2])$. The central feature of the CMS apparatus
24 is a superconducting solenoid, of 6 m internal diameter. Within the field volume are
25 the silicon pixel and strip tracker, and the barrel and endcap calorimeters ($|\eta| < 3$): a
26 crystal electromagnetic calorimeter (ECAL) and a brass-scintillator hadronic calorimeter
27 (HCAL). Outside the field volume, in the forward region, there is an iron-quartz fiber
28 hadronic calorimeter ($3 < |\eta| < 5$). The HCAL and ECAL cells are grouped into tow-

29 ers, projecting radially outward from the origin, for triggering purposes and to facilitate
 30 the jet reconstruction. In the region $|\eta| < 1.74$ these projective calorimeter towers have
 31 segmentation $\Delta\eta = \Delta\phi = 0.087$, and the η and ϕ width progressively increases at higher
 32 values of η . The energy in the HCAL and ECAL within each projective tower is summed
 33 to find the calorimeter tower energy. Towers with $|\eta| < 1.3$ contain only cells from the
 34 barrel calorimeters, towers in the transition region $1.3 < |\eta| < 1.5$ contain a mixture of
 35 barrel and endcap cells, and towers in the region $1.5 < |\eta| < 3.0$ contain only cells from
 36 the endcap calorimeters.

37 Jets are reconstructed using both the iterative and midpoint cone algorithms [5], with
 38 indistinguishable results for this analysis. Below we will discuss three types of jets: recon-
 39 structed, corrected and generated. The reconstructed jet energy, E , is defined as the scalar
 40 sum of the calorimeter tower energies inside a cone of radius $\sqrt{(\Delta\eta)^2 + (\Delta\phi)^2} = 0.5$, cen-
 41 tered on the jet axis. The jet momentum, \vec{p} , is the corresponding vector sum: $\vec{p} = \sum E_i \hat{u}_i$
 42 with \hat{u}_i being the unit vector pointing from the origin to the energy deposition E_i inside
 43 the cone. The jet transverse momentum, p_T , is the component of \vec{p} in the transverse
 44 plane. The E and \vec{p} of a reconstructed jet are then corrected for the non-linear response
 45 of the calorimeter to a generated jet. Generated jets come from applying the same jet
 46 algorithm to the Lorentz vectors of stable generated particles before detector simulation.
 47 On average, the p_T of a corrected jet is equal to the p_T of the corresponding generated jet.
 48 The corrections estimated from a GEANT [6] simulation of the CMS detector increase the
 49 average jet p_T by roughly 50% (10%) for 70 GeV (3 TeV) jets in the region $|\eta| < 1.3$. Fur-

50 ther details on jet reconstruction and jet energy corrections can be found elsewhere [5, 7].
51 The jet measurements presented here are within the region $|\eta| < 1.3$, where the sensitivity
52 to new physics is expected to be the highest, and where the reconstructed jet response
53 variations as a function of η are both moderate and smooth.

54 The dijet system is composed of the two jets with the highest p_T in an event (leading
55 jets), and the dijet mass is given by $m = \sqrt{(E_1 + E_2)^2 - (\vec{p}_1 + \vec{p}_2)^2}$. The estimated dijet
56 mass resolution varies from 9% at a dijet mass of 0.7 TeV to 4.5% at 5 TeV.

57 CMS will record events that pass a first level trigger followed by a high level trigger. For
58 an instantaneous luminosity of $10^{32} \text{ cm}^{-2}\text{s}^{-1}$, we consider three event samples collected
59 by requiring at least one jet in the high level trigger with corrected transverse energy
60 above 60, 120 and 250 GeV, prescaled by factors of 2000, 40 and 1, respectively. For
61 an integrated luminosity of 100 pb^{-1} , the three event samples will effectively correspond
62 to 0.05, 2.5, and 100 pb^{-1} . The first event sample will be used to measure the trigger
63 efficiency of the second sample. The second and third event samples will be used to study
64 dijets of mass above 330 and 670 GeV, respectively, for which the trigger efficiencies are
65 expected to be higher than 99% [8].

66 Backgrounds from cosmic rays, beam halo, and detector noise are expected to occasion-
67 ally produce events with large or unbalanced energy depositions. They will be removed
68 by requiring $\cancel{E}_T / \sum E_T < 0.3$ and $\sum E_T < 14 \text{ TeV}$, where \cancel{E}_T ($\sum E_T$) is the magnitude of
69 the vector (scalar) sum of the transverse energies measured by all calorimeter towers in
70 the event. This cut is estimated to be more than 99% efficient for both QCD jet events

71 and the signals of new physics considered. In the high p_T region relevant for this search,
72 jet reconstruction is fully efficient.

73 CMS plans to search for contact interactions using the jet p_T distribution. Figure 1
74 shows the inclusive jet differential cross section as a function of p_T , for jets with $|\eta| <$
75 1. Considering first the QCD processes, the reconstructed and corrected quantities are
76 compared with the QCD prediction for generated jets. After corrections, the reconstructed
77 and generated distributions agree. The ratio of the corrected jet cross section to the
78 generated jet cross section varies between 1.2 at $p_T = 100$ GeV and 1.05 at $p_T = 500$
79 GeV, remaining roughly constant for higher p_T . The deviation of this ratio from 1 is
80 attributed to the smearing effect of the jet p_T resolution on the steeply falling spectrum.
81 The measured spectrum in data could be further corrected for resolution smearing, and
82 this ratio from simulation is an estimate of the size of that correction. The measurement
83 uncertainties are predominantly systematic. The inset in Fig. 1 shows the effect on the jet
84 rate of a 10% uncertainty in the jet energy correction. This level of uncertainty could be
85 expected in early running, for an integrated luminosity around 10 pb^{-1} . This experimental
86 uncertainty is roughly ten times larger than the uncertainties from parton distributions,
87 as estimated using CTEQ6.1 fits [9]. Figure 1 shows that the effect of new physics from a
88 contact interaction with scale $\Lambda^+ = 3$ TeV is convincingly above what could be expected
89 for measurement uncertainties with only 10 pb^{-1} . For comparison, a Tevatron search has
90 excluded contact interactions with scales Λ^+ below 2.7 TeV [10].

91 CMS plans to search for narrow dijet resonances using the dijet mass distribution.

92 Figure 2 shows the differential cross section versus dijet mass, where both leading jets
 93 have $|\eta| < 1$, and the mass bins have a width roughly equal to the dijet mass resolution.
 94 Considering first the QCD processes, the cross section for corrected jets agrees with the
 95 QCD prediction from generated jets. To determine the background shape either the Monte
 96 Carlo prediction or a parameterized fit to the data can be used. The inset to Fig. 2 shows a
 97 simulation of narrow dijet resonances with a q^* production cross section. This is compared
 98 to the statistical uncertainties in the QCD prediction, including trigger prescaling. This
 99 comparison shows that with an integrated luminosity of 100 pb^{-1} a q^* dijet resonance with
 100 a mass of 2 TeV would produce a convincing signal above the statistical uncertainties from
 101 the QCD background. For comparison, a Tevatron search has excluded q^* dijet resonances
 102 with mass, M , below 0.87 TeV [11]. The heaviest dijet resonances that CMS can discover
 103 (at five standard deviations) with 100 pb^{-1} of integrated luminosity, using this search
 104 technique and including the expected systematic uncertainties [12, 13], are: 2.5 TeV for
 105 q^* , 2.2 TeV for axiguons [14] or colorons [15], 2.0 TeV for E_6 diquarks [16], and 1.5 TeV
 106 for color octet technirhos [17]. Studies of the jet η cut have concluded that the optimal
 107 sensitivity to new physics is achieved with $|\eta| < 1.3$ for a 2 TeV spin 1 dijet resonance
 108 decaying to $q\bar{q}$ [18].

109 CMS plans to search for both contact interactions and dijet resonances using the dijet
 110 ratio, $r = N(|\eta| < 0.7)/N(0.7 < |\eta| < 1.3)$, where N is the number of events with both jets
 111 in the specified $|\eta|$ region. The dijet ratio is sensitive to the dijet angular distribution. For
 112 the QCD processes, the dijet ratio is the same for corrected jets and generated jets, and is

113 constant at $r = 0.5$ for dijet masses up to 6 TeV [18]. Figure 3 shows the dijet ratio from
 114 contact interactions and dijet resonances, compared to the expected statistical uncertainty
 115 on the QCD processes, for 100 pb^{-1} of integrated luminosity, including trigger prescaling.
 116 The signal from a contact interaction with scale $\Lambda^+ = 5 \text{ TeV}$ rises well above the QCD
 117 statistical errors at high dijet mass. Systematic uncertainties in the dijet ratio are expected
 118 to be small, since they predominantly cancel in the ratio as previously reported [12, 19].
 119 Using the dijet ratio, CMS can discover a contact interaction at scale $\Lambda^+ = 4, 7$ and 10
 120 TeV with integrated luminosities of 10, 100, and 1000 pb^{-1} , respectively [18]. The signal
 121 from a 2 TeV spin $1/2$ q^* produces a convincing peak in the dijet ratio, because it has
 122 a significant rate and a relatively isotropic angular distribution compared to the QCD
 123 t -channel processes. Fixing the cross section of the 2 TeV dijet resonance for $|\eta| < 1.3$
 124 at 13.6 pb (from the q^* model), the dijet ratio in the presence of QCD background
 125 increases by approximately 6% when considering a spin 2 resonance decaying to both
 126 $q\bar{q}$ and gg (such as a Randall-Sundrum graviton [20]), and the dijet ratio decreases by
 127 approximately 4% when considering a spin 1 resonance decaying to $q\bar{q}$ (such as a Z' ,
 128 axigluon, or coloron) [18]. Hence, the sensitivity to a 2 TeV dijet resonance depends only
 129 weakly on the spin of the resonance. To measure the spin, we need both the dijet ratio and
 130 an independent measurement of the cross section of the resonance, for example, from the
 131 dijet mass differential cross section. Nevertheless, with sufficient luminosity, this simple
 132 measure of the dijet angular distribution, or a more complete evaluation of the angular
 133 distribution, can be used to see these small variations and infer the spin of an observed

134 dijet resonance.

135 In conclusion, CMS plans to use measurements of rate as a function of jet p_T and dijet
136 mass, as well as a ratio of dijet rates in different η regions, to search for new physics in the
137 data sample collected during early LHC running. With integrated luminosity samples in
138 the range 10–100 pb⁻¹, CMS will be sensitive to contact interactions and dijet resonances
139 beyond those currently excluded by the Tevatron.

140 We thank the technical and administrative staffs at CERN and other CMS Institutes,
141 and acknowledge support from: FMSR (Austria); FNRS and FWO (Belgium); CNPq and
142 FAPERJ (Brazil); MES (Bulgaria); CERN; CAS and NSFC (China); MST (Croatia);
143 University of Cyprus (Cyprus); Academy of Sciences and NICPB (Estonia); Academy of
144 Finland, ME and HIP (Finland); CEA and CNRS/IN2P3 (France); BMBF and DESY
145 (Germany); GSRT (Greece); NKTH (Hungary); DAE and DST (India); IPM (Iran); UCD
146 (Ireland); INFN (Italy); KICOS (Korea); CINEVESTAV, CONACYT and UASLP-FAI
147 (Mexico); PAEC (Pakistan); SCSR (Poland); FCT (Portugal); JINR (Armenia, Belarus,
148 Georgia, Ukraine, Uzbekistan); MST and MAE (Russia); MSEP (Serbia); OCT (Spain);
149 ETHZ, PSI, University of Zurich (Switzerland); NSC (Taipei); TUBITAK and TAEK
150 (Turkey); STFC (United Kingdom); DOE and NSF (USA).

151 **References**

152 [1] E. Eichten, K. Lane and M. E. Peskin, Phys. Rev. Lett. **50**, 811 (1983).

- 153 [2] U. Baur, I. Hinchliffe and D. Zeppenfeld, *Int. J. Mod. Phys.* **A2**, 1285 (1987).
- 154 [3] T. Sjostrand, L. Lonnblad, S. Mrenna, hep-ph/0108264.
- 155 [4] CMS Collaboration, “The CMS experiment at the CERN LHC” (accepted for publi-
156 cation in JINST).
- 157 [5] CMS Collaboration, Physics TDR Volume I, CERN-LHCC-2006-001.
- 158 [6] S. Agostinelli *et al.* (GEANT4 Collaboration), *Nucl. Instrum. Meth.* **A506**, 250 (2003).
- 159 [7] CMS Collaboration, CMS Physics Analysis Summary JME-07-003 (2008). at
160 <http://cms-physics.web.cern.ch/cms-physics/public/JME-07-003-pas.pdf> .
- 161 [8] S. Esen and R. Harris, CMS Note 2006/069.
- 162 [9] J. Pumplin *et al.* (CTEQ Collaboration), *JHEP* **07**, 012 (2002).
- 163 [10] B. Abbott *et al.* (D0 Collaboration), *Phys. Rev. Lett.* **82**, 2457 (1999).
- 164 [11] K. Hatakeyama *et al.* (CDF Collaboration) recent public results at
165 http://www-cdf.fnal.gov/physics/exotic/r2a/20080214.mjj_resonance_1b/.
- 166 [12] CMS Collaboration, *J. Phys. G: Nucl. Part. Phys.* **34**, 995 (2006).
- 167 [13] K. Gumus, N. Akchurin, S. Esen and R. Harris, CMS Note 2006/070.
- 168 [14] J. Bagger, C. Schmidt and S. King, *Phys. Rev.* **D37**, 1188 (1988).
- 169 [15] E. Simmons, *Phys. Rev.* **D55**, 1678 (1997).

170 [16] J. Hewett and T. Rizzo, Phys. Rep. **183**, 193 (1989) and references therein.

171 [17] K. Lane and S. Mrenna, Phys. Rev. **D67**, 115011 (2003).

172 [18] CMS Collaboration, CMS Physics Analysis Summary SBM-07-001 (2007) at

173 <http://cms-physics.web.cern.ch/cms-physics/public/SBM-07-001-pas.pdf> .

174 [19] S. Esen and R. Harris, CMS Note 2006/071.

175 [20] L. Randall and R. Sundrum, Phys. Rev. Lett. **83**, 3370 (1999).

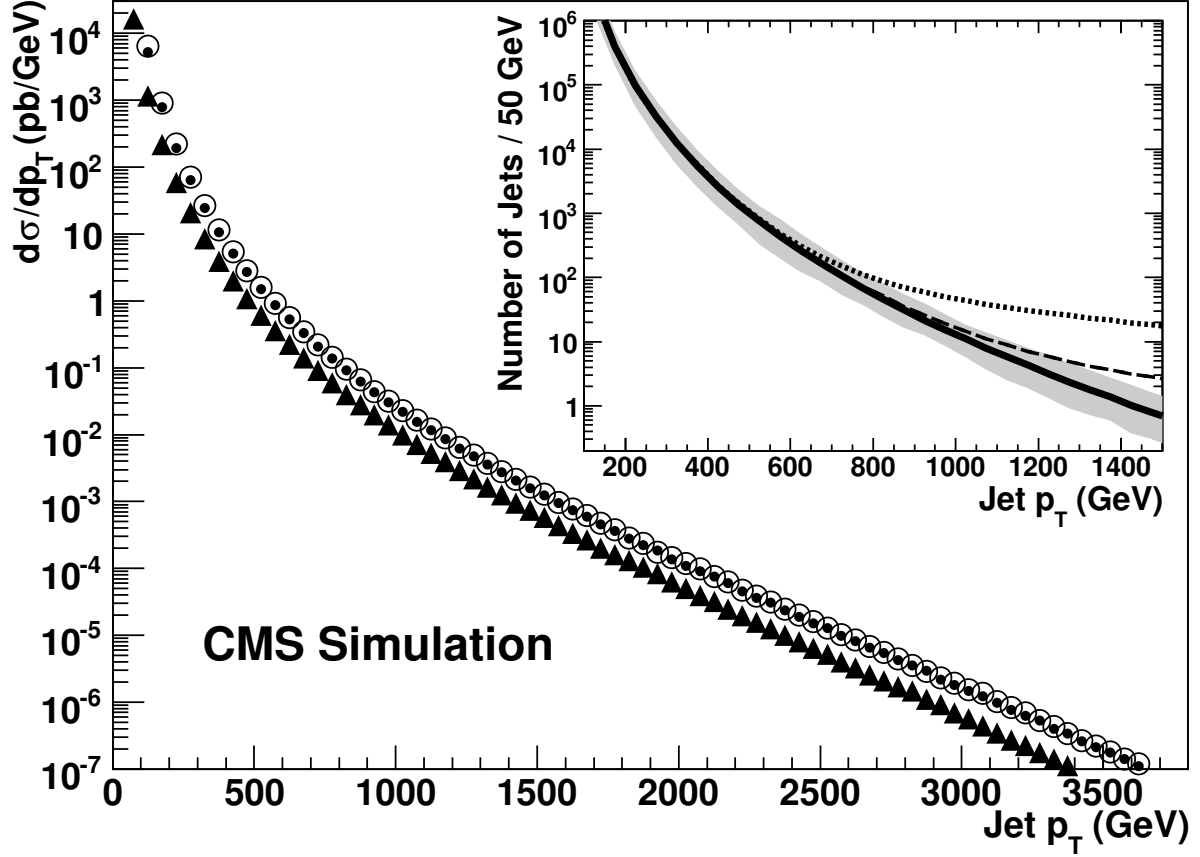


Figure 1: The inclusive jet p_T differential cross section expected from QCD for $|\eta| < 1$, for generated jets (points), reconstructed jets (triangles), and corrected jets (open circles). The inset shows the number of generated jets expected in 50 GeV bins for an integrated luminosity of 10 pb^{-1} . The standard QCD curve (solid) is modified by a signal from contact interactions with scale $\Lambda^+ = 3 \text{ TeV}$ (dotted) and 5 TeV (dashed). The shaded band represents the effect of a 10% uncertainty on the jet energy scale.

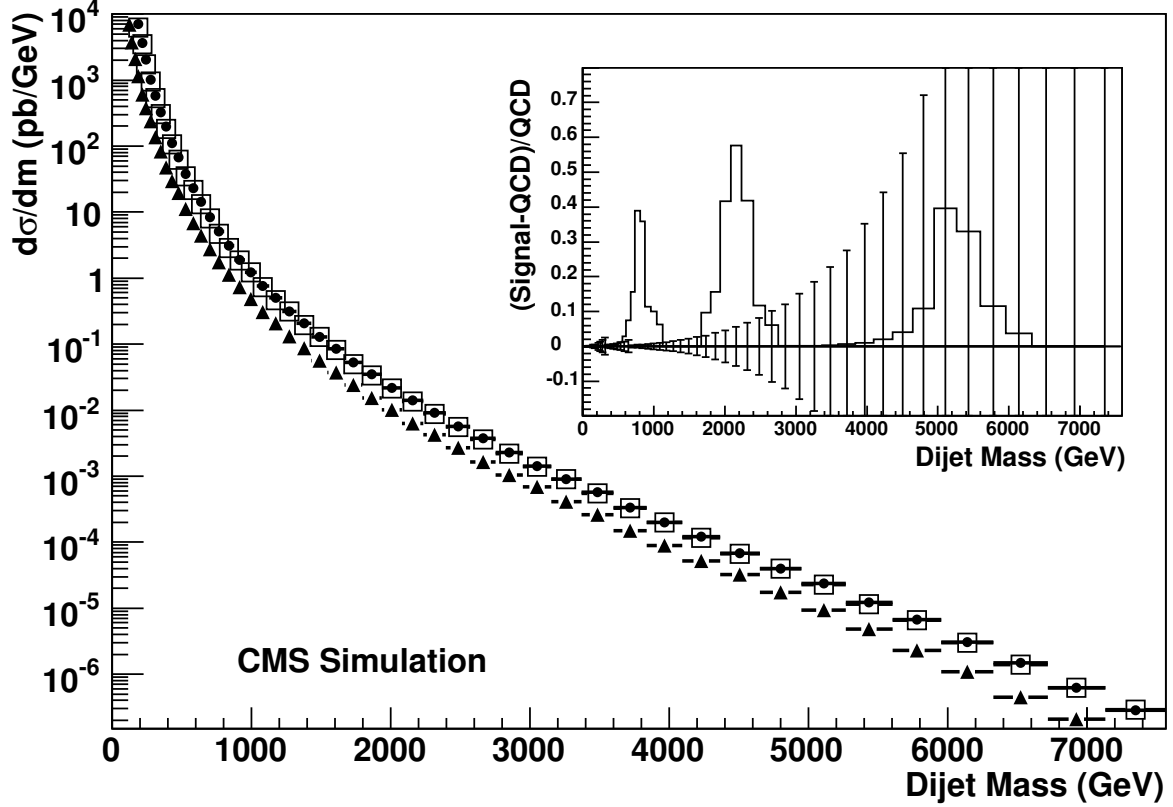


Figure 2: The dijet mass differential cross section expected from QCD for $|\eta| < 1$ from generated jets (points), reconstructed jets (triangles), and corrected jets (open boxes). The inset shows dijet resonances reconstructed using corrected jets, coming from q^* signals [13] of mass 0.7, 2, and 5 TeV. The fractional difference (histogram) between the q^* signal and the QCD background is compared to the statistical uncertainties in the QCD prediction (vertical bars) for an integrated luminosity of 100 pb^{-1} .

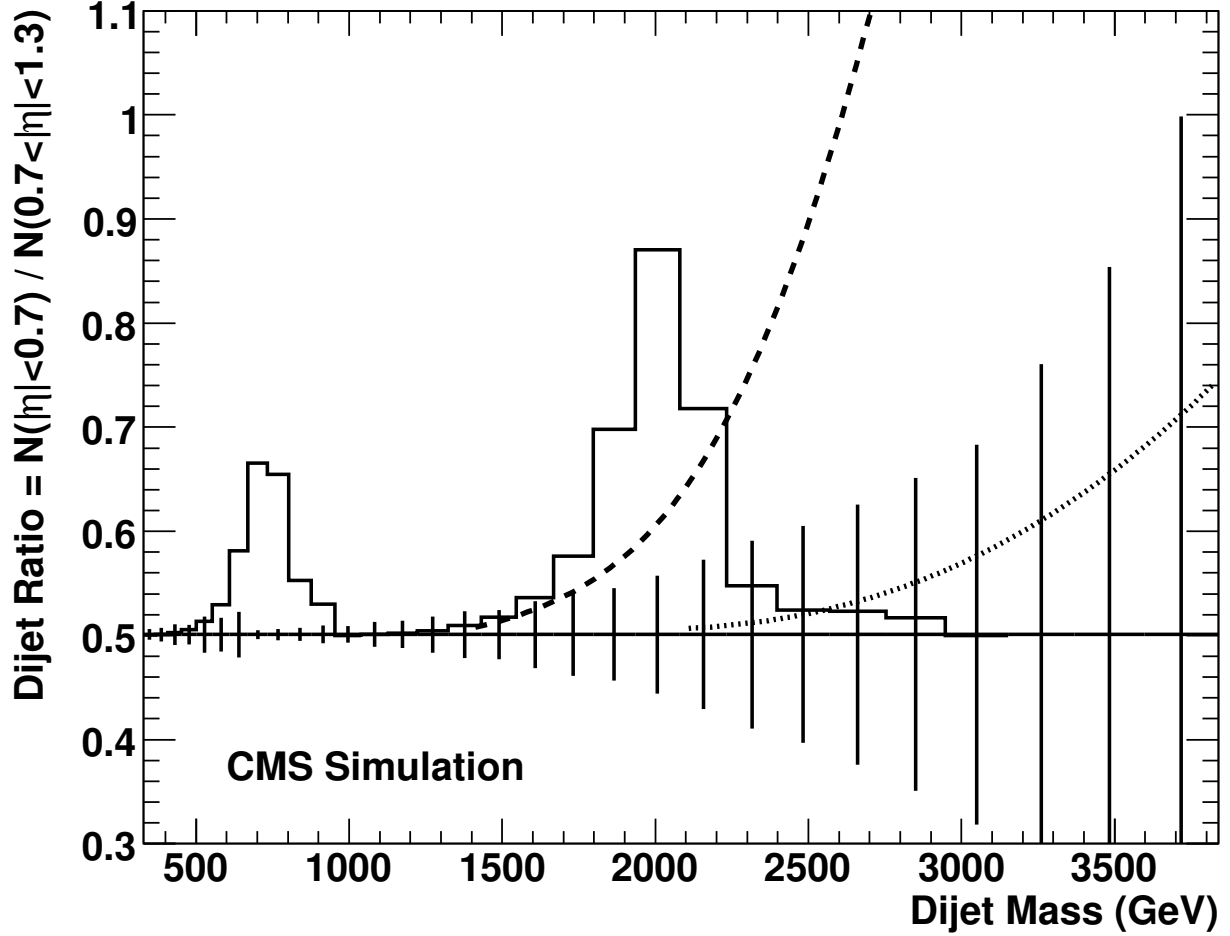


Figure 3: The dijet ratio for corrected jets expected from QCD (horizontal line), with statistical uncertainties (vertical bars) for an integrated luminosity of 100 pb^{-1} , is compared to QCD + contact interaction signals with a scale $\Lambda^+ = 5 \text{ TeV}$ (dashed) and 10 TeV (dotted), as well as to QCD + dijet resonance signals (histogram) with q^* masses of 0.7 and 2 TeV .